ELSEVIER

Journal of Nuclear Materials 241–243 (1997) 569–573

journal of nuclear materials

Effects of edge and central fuelling on particle confinement in JT-60U

H. Takenaga *, N. Asakura, K. Shimizu, K. Nagashima, H. Kubo, A. Sakasai

Naka Fusion Research Establishment, Japan Atomic Energy Research Institute, Naka-machi, Naka-gun, Ibaraki-ken 311-01, Japan

Abstract

In order to understand the effects of the particle source distribution on the global particle confinement, the particle balance in JT-60U has been quantitatively analyzed. The dependence of the particle confinement time on the ratio of the central fuelling due to NBI to the edge fuelling due to wall recycling and gas-puffing was investigated. It was found that the particle confinement time increased with this ratio for the L-mode and ELMy H-mode plasmas, while, for the ELM-free H-mode plasma, the dependence of the particle confinement time on this ratio was not obvious. Furthermore, the confinement times of the center and edge fuelled particles were separated for the L-mode plasma. It was also found that the confinement time of the center fuelled particles was about 3 times longer than that of the edge fuelled particles.

Keywords: JT-60U; Tokamak; Particle fuelling; Particle transport and confinement; Particle balance

1. Introduction

Particle confinement is an indispensable factor for the design of a fusion reactor, as well as energy confinement, from its relation to the plasma density control and helium ash exhaust. The scaling law of the energy confinement time has been established in the L-mode plasma [1] and afterwards energy confinement of the improved confinement modes was well studied [2]. In contrast, only a few databases of particle confinement have been presented [3]. The task to establish the scaling law of the particle confinement time started for ITER physics R&D. However, the dependence of the particle confinement time on the plasma parameters has not been understood sufficiently. The fact that the understanding of particle confinement stays behind the understanding of energy confinement is chiefly caused by the variety of particle source distributions. The auxiliary heating power is mostly injected in the central region. On the other hand, particles are supplied not only in the central region by NBI but also in the edge region by wall recycling and gas-puffing. With increasing NBI injection power and with progress in wall conditioning such as glow discharge cleaning (GDC) and boronization, the particle fuelling rate due to NBI increases and the particle fuelling rate due to wall recycling decreases. Therefore, the fuelling rate of NBI becomes comparable to, or larger than, that of wall recycling. The ratio between the fuelling rate of NBI and wall recycling is closely related to the particle source distribution and this ratio must affect the global particle confinement. For the particle confinement study, it is important to achieve a systematic understanding of the database with its variety in particle source distributions.

In this paper, we analyze the particle balance quantitatively for the L-mode, ELM-free H-mode and ELMy H-mode plasmas of JT-60U, so as to understand the effects of the particle source distribution. The dependence of the particle confinement time on the ratio of the central fuelling to the edge fuelling has been investigated and the confinement times of the center and edge fuelled particles are separated.

2. Analysis of global particle balance

2.1. Method of analysis

The particle balance equation can be expressed using the particle confinement time (τ_p) as follows.

$$\frac{dN_e}{dt} = -\frac{N_e}{\tau_p} + S_R + S_{GP} + S_{NB}, \quad (1)$$

* Corresponding author. Tel.: +81-29 270 7343; fax: +81-29 270 7449; e-mail: takenaga@naka.jaeri.go.jp.

PII S0022-3115(96)00566-1

where N_e is the total electron number in the main plasma, S_R, S_{GP} and S_{NB} are the particle fuelling rate in the main plasma due to wall recycling, gas-puffing and NBI, respectively.

The values of S_R and S_{GP} were estimated through the calculation of the neutral particle penetration rate into the main plasma using the neutral particle transport simulation code DEGAS [4]. Details of this method have already been reported [5]. Here, its essential features are summarized as follows. The electron density, the electron temperature and the ion temperature at the divertor region and SOL were calculated using an interpretative simple divertor code [6]. This code solves 1D fluid equations along the magnetic field. The measured values of the electron density and temperature at the divertor plates using Langmuir probes were used as the boundary condition. The Dα emission profile calculated with DEGAS was fitted to the measured profile so as to determine the absolute value of S_R. The Dα emission intensities were measured with a fiber array which cover the whole poloidal cross-section. The neutral particles were released only at the divertor plates, because the wall source is much smaller than the divertor source. The absolute value of S_{GP} was determined from the gas flow rate through the gas-puffing port. The absolute errors in S_R and S_{GP} were estimated to be about 40% and also the relative errors were estimated to be 10%. These errors mainly come from uncertainty of the probe data. The value of S_{NB} was estimated from the injection power and the beam energy and its distribution was calculated using the orbit following Monte-Carlo (OFMC) code [7].

In the analyses we assumed that $Z_{eff} = 1$. If we take the density of fully stripped carbon and oxygen in the main plasma to be 2–3% of the electron density ($Z_{eff} < 4$), as is observed in typical NBI heated plasmas of JT-60U, τ_p becomes smaller by 30–40%.

2.2. Results of analysis

The analyses were performed for the L-mode, ELM-free H-mode and ELMy H-mode plasmas with a wide range of $S_{NB}/(S_R + S_{GP})$. Fig. 1 shows an example of the particle source distributions for the L-mode plasma with plasma current $I_p = 2$ MA, magnetic field $B_T = 3.5$ T line averaged density $\bar{n}_e = 2 \times 10^{19}$ m^{-3} and net heating power $P_{net} = 5$ MW. The fuelling rate of wall recycling was substantial in the peripheral region of $r/a > 0.95$, while, the fuelling rate of NBI was relatively flat and was dominant in the central region of $r/a < 0.4$.

In Fig. 2, the values of S_{NB} are plotted against $S_R + S_{GP}$ for the L-mode plasmas with $I_p = 1.8$–3 MA, $B_T = 3$–4 T, $\bar{n}_e = 1$–4×10^{19} m^{-3} and $P_{net} = 5$–16 MW, for the ELM-free H-mode plasmas ($I_p = 2$–3 MA, $B_T = 4$ T, $\bar{n}_e = 1$–3×10^{19} m^{-3}, $P_{net} = 13$–18 MW) and for the ELMy H-mode plasmas ($I_p = 1.2$ MA, $B_T = 2$ T, $\bar{n}_e = 2$–3×10^{19} m^{-3}, $P_{net} = 13$–20 MW). The error bar shown in this figure shows the absolute error of S_R, S_{GP} and S_{NB}

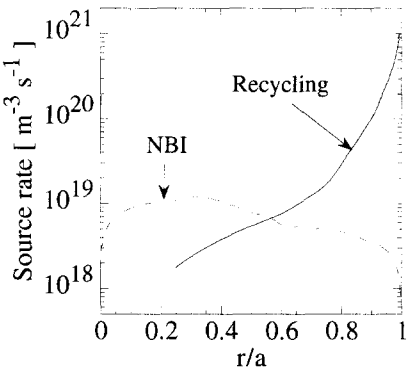

Fig. 1. Particle source distributions calculated with DEGAS and OFMC. Solid line shows particle source due to wall recycling and dashed line shows particle source due to NBI.

calculations. In the DEGAS calculation for the ELMy H-mode plasma, the density and temperature at the divertor plates, which are the boundary condition for the simple divertor code as mentioned in Section 2.1, were estimated using the data of the Langmuir probes during the periods between ELM pulses. The averaged values of Dα emission intensity in the ELMy phase were used to determine the absolute value of S_R. The particle flux to the divertor plates is larger during the ELM pulse than between the ELM pulses, hence, the divertor density must be larger during the ELM pulse than between the ELM pulses. Then, S_R might be overestimated because the penetration rate of the neutral particle into the main plasma is smaller during the ELM pulses than between the ELM pulses due to strong shielding effect of the high density in the divertor region. If the Dα emission intensities during the periods between ELM pulses were used, S_R becomes smaller by

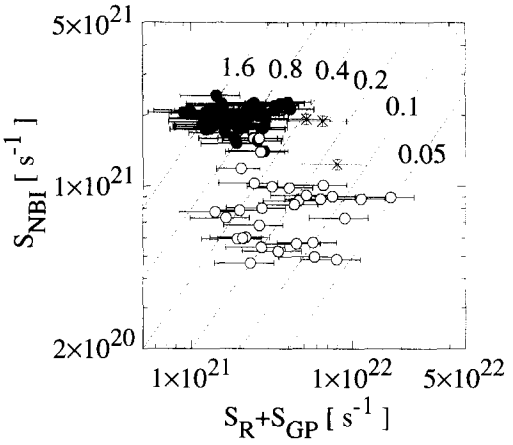

Fig. 2. Relationship between S_{NB} and $S_R + S_{GP}$. Open circles, closed circles and cross symbols show the data for L-mode, ELM-free H-mode and ELMy H-mode plasmas, respectively. Solid lines show constant values of $S_{NB}/(S_R + S_{GP})$.

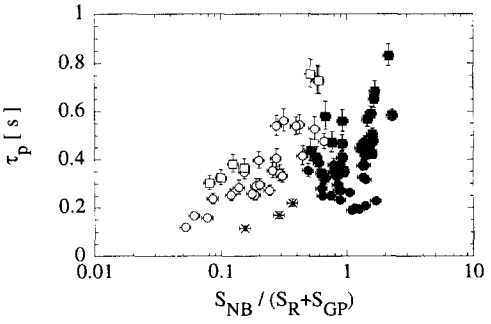

Fig. 3. Correlation between τ_p and $S_{NB}/(S_R + S_{GP})$. Open circles and open squares show the data of L-mode plasma for $I_p = 1.8$–2 MA and $I_p = 3$ MA, respectively. Closed circles and closed squares show the data of ELM-free H-mode plasma for $I_p = 2$ MA and $I_p = 3$ MA, respectively. Cross symbols show the data of ELMy H-mode of $I_p = 1.2$ MA.

30–50%. The ratio of $S_{NB}/(S_R + S_{GP})$ is estimated to be 0.05–0.6 for the L-mode plasmas, 0.5–2 for the ELM-free H-mode plasmas and 0.1–0.5 for the ELMy H-mode plasmas.

The relationship between τ_p and $S_{NB}/(S_R + S_{GP})$ is shown in Fig. 3. The error bar shows the uncertainty in τ_p and $S_{NB}/(S_R + S_{GP})$ due to the relative errors of S_R and S_{GP}. The values of τ_p increase with $S_{NB}/(S_R + S_{GP})$ for the L-mode plasma, both for $I_p = 1.8$–2 MA (open circles) and $I_p = 3$ MA (open squares), and τ_p seems to depend on I_p. In the previous analyses in JT-60U, τ_p decreased with increasing $\bar{n}_e$ for the low power NBI heated L-mode plasma and τ_p increased with $\bar{n}_e$ for the high power NBI heated L-mode plasma [5]. However, this difference can be understood in terms of the dependence on $S_{NB}/(S_R + S_{GP})$.

In the ELMy H-mode ($I_p = 1.2$ MA), τ_p also tends to increase with $S_{NB}/(S_R + S_{GP})$. The values of τ_p for the ELMy H-mode plasmas are smaller than those for the L-mode plasmas, even though the overestimation of S_R as mentioned above was taken into account. One of the reasons could be the I_p dependence of τ_p. As another reason, we point out the effect of the edge density on the separatrix. The edge density of the ELMy H-mode plasma was smaller than that of the L-mode plasma for the same value of $\bar{n}_e$. The edge density affects the main plasma density, because the edge density is a boundary condition of the density profile in the main plasma. Even if there is no particle source in the main plasma, the electron number in the main plasma becomes finite when the edge density is not zero. Therefore, τ_p becomes large when the edge density is high. This effect has to be clarified in further work.

In the ELM-free H-mode plasma, the dependence of τ_p on $S_{NB}/(S_R + S_{GP})$ is not obvious. For the data of $I_p = 3$ MA (closed squares), it seems that τ_p depends on $S_{NB}/(S_R + S_{GP})$, however, for the data of $I_p = 2$ MA (closed circles), this dependence is not clear. The dependence of τ_p on $\bar{n}_e$ was reported for ohmically heated plasmas in four tokamaks [8]. They showed that τ_p increased with $\bar{n}_e$ up to a certain threshold value of $\bar{n}_e$ and decreased with $\bar{n}_e$ above this value. The dependence of τ_p on $\bar{n}_e$ for the high $\bar{n}_e$ region was explained by the particle source distribution localized at the plasma edge. When central fuelling is comparable with edge fuelling, the dependence of τ_p on the source distribution might become weak and a dependence of τ_p on the plasma parameters might be observed. In fact, there is good correlation between τ_p in the ELM-free H-mode analyzed here and $\bar{n}_e$ as reported in Ref. [9]. It is noted that the ranges of the plasma parameters analyzed here are different for the L-mode, ELM-free H-mode and ELMy H-mode plasmas. Systematic investigations have to be performed for many more cases of the plasma parameters in future.

In many plasma experiments, the dependence of τ_p on the plasma parameters such as I_p, $\bar{n}_e$ and P was investigated so as to establish the scaling law of τ_p as well as energy confinement time. The results obtained here show that the dependence of τ_p on the source distribution must be taken into account. In Section 3, the particle balance considering the difference between the central and edge fuelling was discussed.

3. Separation of confinement times of center and edge fuelled particles

3.1. Method of separation

We consider the particle balance for the particles supplied by NBI (central fuelling) and by wall recycling and gas-puffing (edge fuelling), separately, as follows;

$$\frac{dN_e^C}{dt} = -\frac{N_e^C}{\tau_p^C} + S_{NB}, \tag{2}$$

$$\frac{dN_e^E}{dt} = -\frac{N_e^E}{\tau_p^E} + S_R + S_{GP}, \tag{3}$$

$$N_e = N_e^C + N_e^E, \tag{4}$$

where N_e^C and N_e^E are the electron numbers contained in the main plasma supplied by central fuelling and edge fuelling, respectively. τ_p^C and τ_p^E are the confinement times of the center fuelled particles and the edge fuelled particles, respectively.

During a steady state, Eqs. (2)–(4) are rewritten as $N_e = \tau_p^E(S_R + S_{GP}) + \tau_p^C S_{NB}$. This equation means that when there are some data points with the same values of τ_p^E and τ_p^C, a straight line fitted to the data plots of $N_e/(S_R + S_{GP})$ against $S_{NB}/(S_R + S_{GP})$ gives τ_p^C from its gradient and τ_p^E from its intercept.

3.2. Numerical simulation of particle transport

In order to clarify the meaning of the separation of the particle confinement times, the particle transport was simulated using the following equations:

$$\frac{\partial n_e}{\partial t} = -\nabla \cdot \Gamma + s, \tag{5}$$

$$\Gamma = -D \cdot \nabla n_e - v \cdot n_e, \tag{6}$$

where Γ is the particle flux across the magnetic surface, s is the particle source, D is the particle diffusion coefficient and v is the inward pinch velocity. The inward pinch velocity can be expressed as $v = D \cdot C_v \cdot 2r/a^2$. The values of D and C_v were assumed to be spatially constant, for simplicity. The following results are obtained for $D = 0.5$ m^2/s and $C_v = 1$, which values were observed in the gas-puff modulation experiment for the ohmically heated plasma in JT-60U [10]. The boundary condition of $n_e(a) = 0$ is used in this simulation.

Fig. 4(a) and (b) show the calculated electron density profile and the particle source distribution used in the calculations during a steady state phase for the central fuelling and for the edge fuelling, respectively. The volume integrated source rates $S_{central}$ and S_{edge} is assumed to be the same value of 1×10^{21}/s. The values of τ_p were estimated to be 0.40 s and 0.045 s for the central and edge fuelling, respectively. They are different for the same transport coefficients due to different source distributions. Then, the calculation was performed for the various ratios of $S_{central}/S_{edge}$. Fig. 5 shows N_e/S_{edge} as a function of $S_{central}/S_{edge}$. The gradient of the straight line fitted to the data of N_e/S_{edge} expresses τ_p for the central fuelling, and

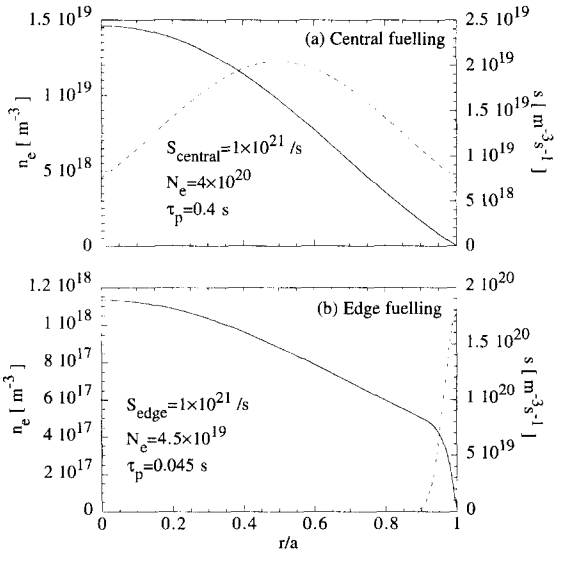

Fig. 4. Calculated electron density profiles (solid line) and source distributions used in the calculations (dashed line) for central fuelling (a) and for edge fuelling (b) in the case of $D = 0.5$ m^2/s and $C_v = 1$.

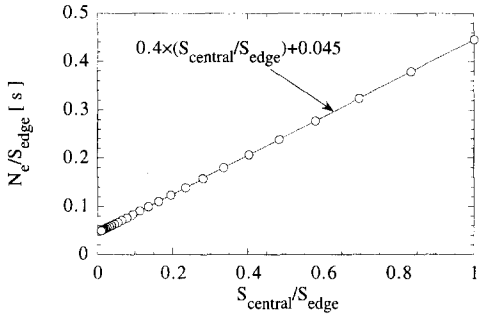

Fig. 5. Calculated N_e/S_{edge} as a function of $S_{central}/S_{edge}$.

intercept expresses τ_p for the edge fuelling, as mentioned in Section 3.1.

3.3. Experimental results and discussion

In order to separate τ_p^C and τ_p^E, the value of $S_{NB}/(S_R + S_{GP})$ was scanned systematically for the L-mode plasma ($I_p = 1.8$ MA, $B_T = 3$ T). The electron density was kept constant ($\bar{n}_e = 2.4 \times 10^{19}$ m^{-3}) using the feedback control system of gas-puffing rate during the scan of NBI power (4–13 MW). The evaluated τ_p decreased with increasing P_{net} in the range of the low P_{net}, however, τ_p increased with P_{net} in the range of the high P_{net}. This data set cannot be understood in terms of the dependence of τ_p on heating power only.

We try to separate the confinement times of the center and edge fuelled particles according to the method mentioned in Section 3.1. Because the NBI power was scanned in this data set, the dependence of τ_p^C and τ_p^E on the heating power must be considered. We assumed the same dependence of τ_p^C and τ_p^E on the net heating power as $\tau_p^{C,E} \propto P_{net}^{-\alpha}$. Therefore, the data plots of $N_e/(S_R + S_{GP})/(P_{net}/8\ \text{MW})^{-\alpha}$ against $S_{NB}/(S_R + S_{GP})$ are expected to lie on the same straight line. When the value of α was taken to be 0.3, the sum of squared errors between the experimental values and the best fitted straight line becomes minimum. When the errors of data were taken into account, the range of $\alpha = 0.2$–0.4 gives acceptable fits. The dependence of τ_p on the heating power in JT-60 has been reported in Ref. [3] as $\tau_p \propto P^{-0.5}$. The dependence obtained here is weaker than that in Ref. [3]. Fig. 6 shows the experimental data plots and the best fitted straight line. The best fitted line gives 1.0 s for $\tau_p^C(P_{net} = 8$ MW) and 0.33 s for $\tau_p^E(P_{net} = 8$ MW), respectively and the ratio of τ_p^C/τ_p^E is estimated to be about 3. The dashed lines in Fig. 6 show the extent of uncertainty in the fitting process when the relative error of S_R and the uncertainty of α are taken into account. This extent yields the ranges of the uncertainty of τ_p^C and τ_p^E as $\pm 30\%$. If we take the density of fully stripped carbon and oxygen in the main plasma to be 2–3% of the electron density, as in Section 2.1, both of τ_p^C and τ_p^E become smaller by 30–40%. It is shown that the data set can be understood in terms of the

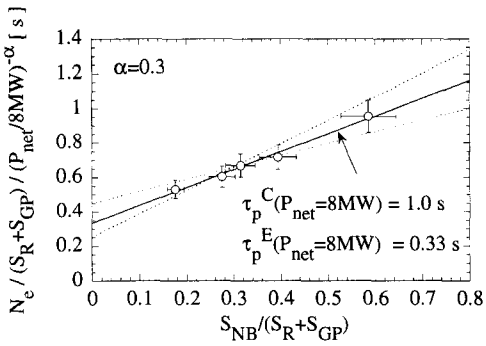

Fig. 6. $[N_e/(S_R + S_{GP})/(P_{net}(8\ MW)^{-\alpha}]$-$[S_{NB}/(S_R + S_{GP})]$ plot. Solid line shows the best fitted line with $\alpha = 0.3$, and dashed lines show the extent of uncertainty due to relative errors of S_R and α.

heating power dependence and the source distribution dependence.

The value of τ_p can be roughly expressed as $\tau_p \approx a\lambda/D$, where a is a minor radius, λ is a penetration depth of the neutral particles and D is a diffusion coefficient. Because the penetration depth of the neutral particles supplied by NBI is about 10 times longer than that supplied by wall recycling, the ratio of τ_p^C/τ_p^E can be roughly estimated to be 10, as in the simulation result of Section 3.2. The experimentally obtained value of τ_p^C/τ_p^E is smaller than this value. This small value comes from the boundary conditions. The out flux across the separatrix from the main plasma to SOL gives the SOL density and this density in SOL raises the base of the density in the main plasma. This raised base of the density gives the small ratio of τ_p^C/τ_p^E.

In order to clarify the effects of the source distribution and the boundary conditions described above, a local transport analysis is useful. A preliminary analysis of the local transport showed τ_p^C and τ_p^E obtained here agree with the values obtained by the local analysis. This will be discussed in a separate paper.

4. Conclusions

The effects of edge and central fuelling on global particle confinement was investigated. It was found that the particle confinement time increased with the ratio of the central fuelling to the edge fuelling for the L-mode and ELMy H-mode plasmas, while, for the ELM-free H-mode plasma, the dependence of the particle confinement time on this ratio was not obvious. The confinement times of the center fuelled particles and the edge fuelled particles were separated for the L-mode plasma for the first time. It was shown that the data set, which can not be understood in terms of heating power dependence only, can be understood in terms of heating power dependence and source distribution dependence. It was also found that the confinement times of the center and edge fuelled particles were estimated to be 1.0 s and 0.33 s, respectively and the confinement time of center fuelled particles was 3 times longer than that of the edge fuelled particles. A database of the particle confinement should include the source distribution and the edge density for the systematic understanding of the particle confinement.

Acknowledgements

The authors wish to thank Dr. M. Shimada, Dr. M. Kikuchi and Dr. T. Takizuka for valuable discussions. They are also grateful to JT-60 team for supports in the experiments.

References

[1] P.N. Yushmanov et al., Nucl. Fusion 30 (1990) 1999.
[2] ITER H-mode Database Working Group (K. Thomsen et al.), Nucl. Fusion 34 (1994) 131.
[3] S. Tsuji, Fusion Eng. Des. 15 (1992) 311.
[4] D.B. Heifetz, in: Physics of Plasma–Wall Interactions in Controlled Fusion, eds. D.E. Post and R. Behrisch (Plenum, New York, 1986) p. 695.
[5] H. Takenaga et al., J. Nucl. Mater. 220–222 (1995) 429.
[6] K. Shimizu et al., J. Nucl. Mater. 196–198 (1992) 476.
[7] K. Tani et al., J. Phys. Soc. Jpn. 50 (1981) 1726.
[8] A.J. Wootton et al., Plasma Phys. Controll. Fusion 30 (1988) 1479.
[9] H. Takenaga et al., Nucl. Fusion 35 (1995) 853.
[10] K. Nagashima et al., Plasma Phys. Controll. Fusion, to be published.